Measurements of the Second Normal Stress Difference for Star Polymers with Highly Entangled Branches

Chang-Soon Lee, Jules J. Magda,* and Kenneth L. DeVries

Departments of Chemical Engineering, Materials Science, and Mechanical Engineering, University of Utah, Salt Lake City, Utah 84112

Jimmy W. Mays

Department of Chemistry, University of Alabama at Birmingham, Birmingham, Alabama 35294

Received March 2, 1992; Revised Manuscript Received May 19, 1992

ABSTRACT: Steady shear flow rheological properties are investigated for concentrated solutions of anionically polymerized star-branched polyisoprenes. Star polymers under these conditions are already known to have enhanced viscosities and first normal stress differences (N_1) compared to linear polymers of similar radius of gyration at the same concentration. This enhancement is often attributed to the suppression of the reptation relaxation mechanism. The new result demonstrated here is that the *second* normal stress difference (N_2) is also enhanced in magnitude for star polymers with long and entangled branches. In fact, N_2 shows more enhancement than N_1, giving a normal stress ratio $-N_2/N_1$ which is larger for entangled star polymer solutions than for entangled linear polymer solutions. Polymer concentration has also been varied, from the highly entangled regime to the semidilute concentration regime. For both star polymers and linear polymers, the normal stress ratio decreases as the concentration is lowered, a result in accordance with theoretical expectations.

Introduction

Long polymer branches are expected to have a dramatic effect on the diffusional and rheological properties of polymer molecules in concentrated solutions or melts.[1,2] Linear polymer molecules are believed to relax primarily by "reptation" or diffusion along the polymer backbone.[3,4] This relaxation mode should be unavailable to polymer molecules with long branches. Therefore branched polymers are expected to have relaxation times which are *enhanced* in magnitude, relative to the values observed for linear polymers of similar size (i.e. radius of gyration).[5,6]

Experimental support for these ideas has already been obtained from diffusion[7-12] and rheological studies[13-22] of star polymers containing "f" branches of equal length emanating from a single branch point. The steady shear flow rheological results for star polymer solutions can be summarized as follows. Attention has primarily been focused on three steady shear flow properties: the viscosity (η_0), the first normal stress difference coefficient (Ψ_1^0), and recoverable shear compliance ($J_e^0 = \Psi_1^0/2\eta_0^2$). The first two of these properties can be related by molecular theory to the longest relaxation time of the polymer solution, whereas J_e^0 is related to the width of the relaxation time spectrum.[23] At low concentrations where the Rouse–Ham theory applies,[24] star polymers exhibit values for η_0, Ψ_1^0, and J_e^0 which are comparable to values observed for linear polymers with the same radius of gyration.[1,15] At the same value of the molecular weight, star polymers exhibit much lower values for these properties. By contrast, η_0, Ψ_1^0, and J_e^0 values are much larger for star polymers than for linear polymers at high concentrations.[6,13,15,19] This result supports the idea that the reptation relaxation mode is important at high concentrations for linear polymers, and suppressed for star polymers.[5,6] Thus at high concentrations in the enhancement regime, the presence of long polymer branches both increases the average relaxation time and the width of the relaxation time spectrum.[18,25]

The principal goal of this study is to make the first measurements of the second normal stress difference coefficient Ψ_2^0 in the same concentration regime. A polymer/solvent system has been chosen (polyisoprene/tetradecane) for which very careful results have already been published for the enhancement of η_0, Ψ_1^0, and J_e^0.[15] Part of the impetus for the study comes from a recent theoretical analysis[26] which predicts the value of Ψ_2^0/Ψ_1^0 for star polymers, based on a modified tube model with polymer relaxation attributed to arm retraction.[6] Thus the results presented within this paper provide an additional test on molecular models for stress relaxation in entangled polymeric liquids.

The value of Ψ_2^0 is also important in its own right, due to its influence on the susceptibility of polymeric liquids to flow instabilities driven by elasticity.[27] For example, the value of Ψ_2^0 may govern an instability observed at the air/liquid interface in cone-and-plate rheometers known as "edge fracture".[28] If the value of Ψ_2^0 is enhanced in magnitude by the presence of long polymer branches, then star polymers should be unusually susceptible to the edge fracture instability.

Experimental Section

Polymer Synthesis and Characterization. Recent progress in scientific rheology can be attributed in no small part to the study of *model* polymers prepared by living polymerization.[29] Polyisoprene (PIP) has played a major role in this advance, because of its low entanglement molecular weight[23] and its suitability for anionic polymerization. Graessley and co-workers[15] have published rheological results for model polyisoprenes, linear and star, over a wide concentration range including the enhancement regime. In order to use the empirical correlations for η_0 and J_e^0 developed in ref 15, polyisoprenes studied here were chosen to be as similar as possible to those investigated earlier by Graessley et al. Table I lists the characteristics of these polymers. In the first step, branches for the two star polymers ("6A" and "10A" in Table I) were prepared by "living" anionic polymerization techniques using *sec*-butyllithium as initiator and benzene as solvent.[29] Small aliquots of both branch materials ("arms") were removed from the reactors, terminated with methanol, and analyzed by gel permeation chromatography (GPC). These experiments were performed in tetrahydrofuran

0024-9297/92/2225-4744$03.00/0

Table I
Polymer Characteristics

sample	$10^5 M_{span}$[a]	polydispersity of span[b]	$10^5 M_{total}$[a]	f	$[\eta]$,[c] dL/g	k_H[d]	$10^5 M_v$[e]
LL	4.63	1.04	4.63	2	2.72[f]	0.35	4.72
LH	10.0	1.16	10.0	2	4.53[g]	0.35	9.42
6A	5.90	1.04	17.6	5.97	4.26	0.48	17.5
10A	6.40	1.04	32.0	10.0	4.22	0.69	

[a] Weight average molecular weight measured by light scattering. [b] Measured by GPC. [c] Measured in toluene at 34.0 °C. [d] Huggins coefficient. [e] Calculated from Mark–Houwink–Sakurada equations in ref 31. [f] $[\eta]$ = 2.80 in cyclohexane at 25.0 °C. [g] $[\eta]$ = 4.46 in cyclohexane at 25.0 °C.

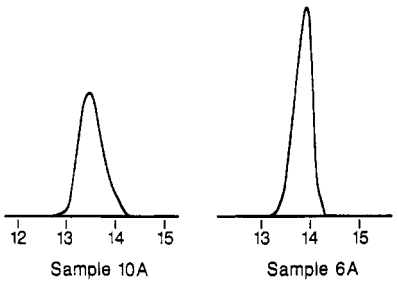

Figure 1. GPC chromatograms for 10-arm and 6-arm star polymers prior to rheological measurements.

using a Waters Associates unit having two "Linear Ultrastyragel" columns in series and a differential refractometer (Model 410) as detector. Calibration was achieved using linear PIP standards purchased from Polymer Laboratories. GPC results indicated molecular weights of about 3.0×10^5 for both arms, with very narrow and symmetrical molecular weight distributions (Table I, column 3). The microstructure of the polyisoprene was examined by NMR and found to conform to that expected for polymers produced by butyllithium-initiated polymerization in benzene (70% cis 1,4; 23% trans 1,4; 7% 3,4 component).

The 6-arm PIP star was produced by adding living polymer in stoichiometric excess to 1,2-bis(trichlorosilyl)ethane (Petrarch Systems Inc., Bristol, PA). The linking agent used for producing the 10-arm star was commercial divinylbenzene (mixed isomers) from Aldrich. After linking was complete, the residual arm was removed by solvent–nonsolvent fractionation (toluene–methanol). GPC results confirmed removal of detectable arm material (Figure 1).

Molecular weights of arm and star PIPs were determined by light scattering measurements in cyclohexane at 25 °C. These measurements employed either a Chromatix KMX-6 low-angle laser light scattering photometer or a Sofica unit modified to incorporate a He–Ne laser. The specific refractive index increment (dn/dc) for PIP at 633 nm under the experimental conditions was measured as 0.105 mL/g using a Chromatix KMX-16 differential refractometer. Results from these measurements are reported in Table I. The branching frequency f in column 5 of Table I was estimated by taking the ratio of the star polymer molecular weight and the branch molecular weight (both taken from light scattering). The nearness of the measured f value for the 6-arm star to the value expected on the basis of the functionality of the linking agent is gratifying. For the 10-arm star, some variation in number of arms is present due to the mechanism of the divinylbenzene linking reaction. Even so, the GPC chromatogram for this material (Figure 1) suggests a narrow polydispersity.

In order to compare rheological properties of star and linear polymers, two linear polyisoprenes of narrow distribution were also investigated ("LL" and "LH" in Table I). The smaller linear polymer was synthesized in our laboratory, whereas the larger linear polymer was purchased commercially.[30] Though this latter polymer is advertised as "monodisperse", GPC and J_e^0 measurements clearly indicate a slightly broader molecular weight distribution for this sample. The ideal linear polymer for the purposes of this paper would have the same rheological properties as a star polymer at lower concentrations, where the effect of branching is slight. As discussed in the Results, this ideal linear polymer would have a molecular weight $M_L \approx 8.6 \times 10^5$, thereby giving the same intrinsic viscosity value in toluene as the star polymer. Thus linear polymer LL is smaller than ideal, and linear polymer LH is somewhat larger than ideal.

Careful intrinsic viscosity results have already been published for linear and 6-arm star polyisoprenes prepared by living polymerization in ref 31. Consequently, it was possible to further characterize our model polymers via the viscosity average molecular weight (Table I, column 8). Significant shear thinning was observed for the star polymer solutions in Ubbelohde capillary viscometers, even of small radii ($r \approx 0.23$ mm). Therefore a Cannon four-bulb capillary viscometer was used to extrapolate measured intrinsic viscosities to the zero shear rate limit (column 6, Table I). Note that the 10-arm star polymer has a slightly *lower* intrinsic viscosity than the 6-arm star, even though the branch size is virtually identical. A similar result has been reported previously in ref 32.

Though polyisoprene star polymers have the experimental advantages described above, they are also susceptible to oxidative degradation at the branch points and at the sites of the double bonds. Consequently, special precautions were taken in preparing the polymer solutions, as described below. Furthermore, GPC measurements were performed on samples both before and *after* rheological measurements. Degradation is also immediately apparent by the dramatic increase it causes in the measured value of J_e^0. Rheological results are presented here only for solutions without significant degradation.

Solution Preparation. Solutions were prepared with the same solvent (tetradecane (TD), bp = 253 °C) and with the same technique as described in ref 15. The enhancement results in ref 15 for the viscosity were also used as a guide in choosing the range of concentrations investigated. The highest polymer concentration (≈24%) was chosen to give significant viscosity enhancement and yet not be too difficult to load into the rheometer. The lowest concentration (≈3%) was determined by the sensitivity limits of the N_2 measurement technique. The highest concentration solution was prepared and studied first rheologically. The same sample was then successively diluted and studied rheologically over a total length of time of approximately 4 weeks. GPC measurements were then performed to test for possible polymer degradation. Rheological measurements were also repeated at the lowest concentration using a fresh sample. Following the approach of ref 15, a volatile solvent (pentane) was used to speed up the dissolution process. First, PIP was completely dissolved in the pentane, and then measured amounts of TD were added to the solution and mixed together slowly. In order to avoid PIP degradation, small amounts of antioxidants (2,6-di-*tert*-butyl-4-methylphenol, Aldrich Chemical Co.) were added to both TD and pentane. The antioxidant concentration was 400 ppm, which is similar to the value reported in ref 15. After complete mixing, pentane was removed from the solution in the following way. While keeping the bottle cap loose, the bottle containing the solution was rotated for 5 days at room temperature and in the dark. Most of the volatile component was removed by vaporization during this period. The small remaining amount of pentane was stripped off under vacuum for 6 h. At no time was the solution temperature allowed to exceed 26 °C, and the solutions were kept in the dark as much as possible. The polymer concentration was calculated by using the densities of the pure components, neglecting volume changes on mixing. Without the use of antioxidants, it was found that as much as 50% of the stars were decomposed into linear polymers, mostly arms. Thus the use of antioxidants is essential for PIP solutions.

Rheometry. Shear flow rheological properties to be investigated are defined as follows:

$$\eta = \tau_{12}/\dot{\gamma} \tag{1}$$

$$\Psi_1 = (\tau_{11} - \tau_{22})/\dot{\gamma}^2 = N_1/\dot{\gamma}^2 \tag{2}$$

$$\Psi_2 = (\tau_{22} - \tau_{33})/\dot{\gamma}^2 = N_2/\dot{\gamma}^2 \tag{3}$$

$$J_e^0 = \Psi_1^0/2\eta_0^2 \tag{4}$$

$$\Psi = -\Psi_2/\Psi_1 \tag{5}$$

where $\dot{\gamma}$ is the shear rate and the stress tensor components τ_{ij} are as defined in ref 33. A zero subscript or superscript on any of these properties denotes the zero-shear-rate limit. The measurements of η, N_1, and N_2 were performed at 25 °C using a Weissenberg R-17 rheogoniometer with cone-and-plate fixtures of diameter 74 mm. This rheometer has been modified to allow accurate N_2 measurements by the placement of miniature pressure transducers at various radial locations along the rheometer plate.[34] The pressure transducers can be used to measure the radial dependence of Π_{22}, the normal component of the total stress tensor in the velocity gradient direction. Typical results obtained for polyisoprene solutions are shown in Figure 2. Figure 2 is a semilogarithmic plot against radial coordinate of $-\Pi_{22} - P_0$, where P_0 is atmospheric pressure. The stress profile in Figure 2 is linear, as expected from a rigorous radial momentum balance given in standard rheometry textbooks.[33] According to this same derivation, the slope of the stress profile is given by $-N_1 - 2N_2$. Since N_1 can be independently measured using a normal force spring attached to the rheometer plate, the value of N_2 can be calculated from the slope of the measured stress profile. This instrument has already been successfully used to measure N_2 for a number of different polymers,[35-37] and additional experimental details are given in refs 34 and 35. The rheometer temperature was controlled within 0.2 °C with a water bath, and measurements were performed using two different cone angles (0.035 and 0.065 radians, respectively). At higher shear rates the shallow cone was used in order to minimize centrifugal forces on the sample.

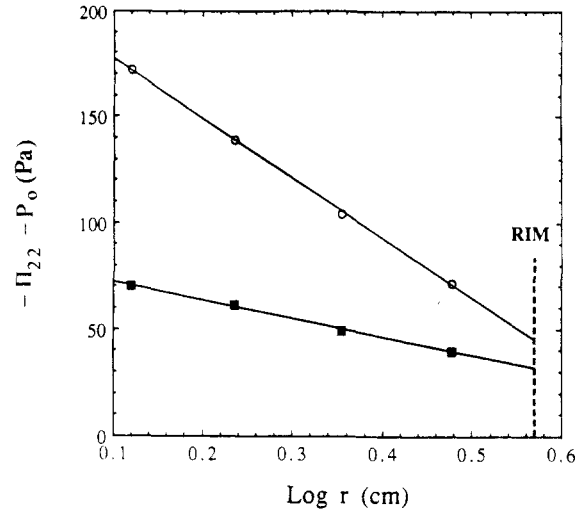

Figure 2. Measured stress profiles for 0.15 g/mL linear (LL, ○) and 0.12 g/mL star polymers (10A, ■). Shear rates are 11.6 and 2.31 L/s for LL and 10A, respectively.

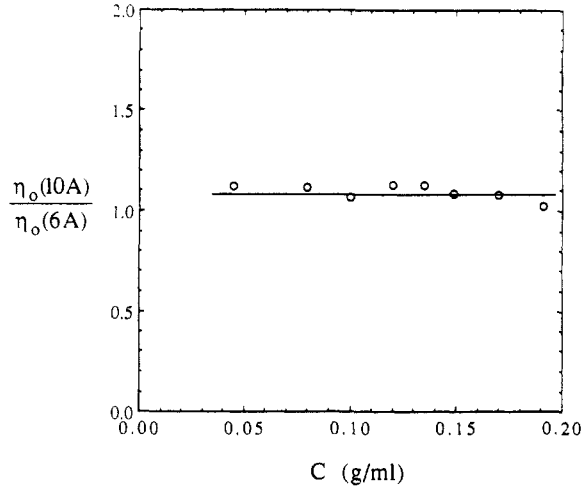

Figure 3. Viscosity ratio between 10-arm and 6-arm star polyisoprenes as a function of polymer concentration in tetradecane.

Results

A. Locating the Enhancement Regime Using Viscosity and Recoverable Compliance Data. We chose our polymer/solvent system in order to take advantage of the published rheological results for polyisoprene molecules (linear and star) presented in ref 15. In this section we demonstrate that our linear polymer results for the viscosity and the compliance are in good agreement with the empirical correlations for these quantities presented in ref 15. By comparing star polymer values for these properties with linear polymer values, we locate the concentration regime within which star polymers and linear polymers relax by different mechanisms. In the next section, new results are presented for the second normal stress difference in this concentration regime.

Figure 3 compares the zero-shear-rate viscosities of the two star polymers in solution, as measured over a wide concentration range encompassing the Rouse regime and the enhancement regime. In the enhancement regime, the viscosity is predicted to depend *exponentially* on the number of entanglements per arm.[6] Light-scattering measurements (Table I) suggest that the arm length is 9% greater for star polymer 10A than for star polymer 6A, and yet the viscosity ratio is close to 1 in Figure 3. Therefore the arm length must be virtually *identical* for the two star polymers, a conclusion which is consistent with GPC measurements made on the arm material. Therefore in figures to follow both star polymers will be assumed to have the same arm length, $M_a \approx 300\,000$.

In the Rouse regime, solution viscosities are predicted to depend on the star polymer radius of gyration (R_g),[24] a prediction which implies a dependence on branch functionality f, since R_g increases with f at constant branch length.[38] However, no dependence on f can be discerned in Figure 3 at any concentration. Alternatively, a close connection between the solution viscosity and the polymer *intrinsic viscosity* has already been pointed out,[1] both for linear polymers and for star polymers with less than three entanglements per branch. By hypothesis, solutions constructed from star polymers and from linear polymers with the same intrinsic viscosity value exhibit similar shear viscosities, provided that the solution is *not* highly entangled. The intrinsic viscosity relation for linear polyisoprenes in toluene is given by[31]

$$[\eta] = 1.72 \times 10^{-5} M_L^{0.74} \tag{6}$$

Here SI units are used and M_L is the molecular weight of linear polyisoprenes. From ref 15, an empirical relation is available for the shear viscosity of linear polyisoprenes in tetradecane:

$$\eta_0 = K_1 C^5 M_L^{3.5} \quad \text{for} \quad CM > \rho M_c \tag{7}$$

Here K_1 is 8.6×10^{-30} when SI units are used. ρ is the polymer density, and M_c is the critical molecular weight at which the melt viscosity starts to show entangled behavior (≈10 000 for polyisoprene[39]). Combination of eq 6 and eq 7 yields an empirical correlation which should be valid for linear polyisoprenes at any concentration and for star polyisoprenes with less than three entanglements

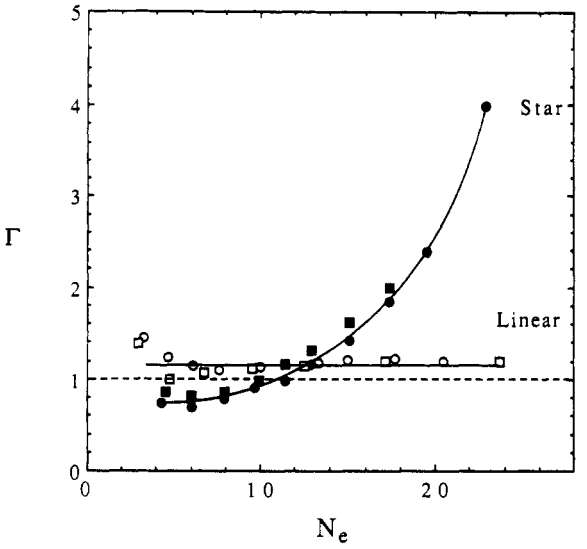

Figure 4. Viscosity enhancement factor (Γ) vs number of entanglements per span (N_e) for linear and star polyisoprenes, indicated by different symbols: LL (○), LH (□), 6A (●), and 10A (■).

per branch:

$$\eta_0 = K_2 C^5 [\eta]^{4.73} \quad (8)$$

Here K_2 is 2.96×10^{-7} for SI units and $[\eta]$ is the intrinsic viscosity in toluene, linear or star. Equation 8 will likely fail for functionalities greater than those studied here, because the intrinsic viscosity begins to decrease with f at constant M_a for f greater than about 18.[32] The viscosity enhancement factor, Γ, is defined as the ratio of the measured solution viscosity to that predicted by eq 8. Figure 4 investigates the dependence of Γ on N_e, the average number of entanglements on the span of a polymer. For both linear and star polyisoprenes, N_e has been calculated from[6]

$$N_e = 2M_a/M_e = 3.84 \times 10^{-4} \phi^{1.21} M_a \quad (9)$$

Here ϕ denotes the polymer volume fraction and M_e the entanglement molecular weight (≈5000 for molten polyisoprene[39]). For both linear polymers, Γ is close to 1 for all values of N_e in Figure 4. This is a reflection of the good agreement which exists between shear viscosities reported here and published correlations such as eq 7. At low concentrations, both star polymers exhibit viscosity enhancement factors close to one in Figure 4. However, once N_e exceeds about 8, Γ begins to increase sharply for the star polymers. Therefore, on the evidence of the viscosity, the reptation relaxation mode becomes unavailable to star polymers when the concentration is high enough to create about 10 or more entanglements per span.

The recoverable shear compliance J_e^0 can also be used to locate the enhancement regime for star polymers. However, one must first ensure that the value of Ψ_1 used to calculate J_e^0 (eq 4) has been accurately extrapolated to zero shear rate. As is well-known,[23] Ψ_1 is more difficult to measure at low shear rates than η. Figure 5 investigates the shear rate dependence of the viscosity and J_e (defined as $\Psi_1/2\eta^2$) for star polymer 6A at a typical concentration. Both quantities are believed to be near their zero-shear-rate limits in Figure 5, because the dimensionless Weissenberg number Wi defined as $J_e^0 \eta_0 \dot{\gamma}$ is exceedingly small ($Wi \approx 0.03$ at the lowest shear rate). Furthermore the extrapolated value of J_e for linear polymers is in good agreement with an empirical correlation for J_e^0 from ref 15, as shown below. At most concentrations, J_e exhibits

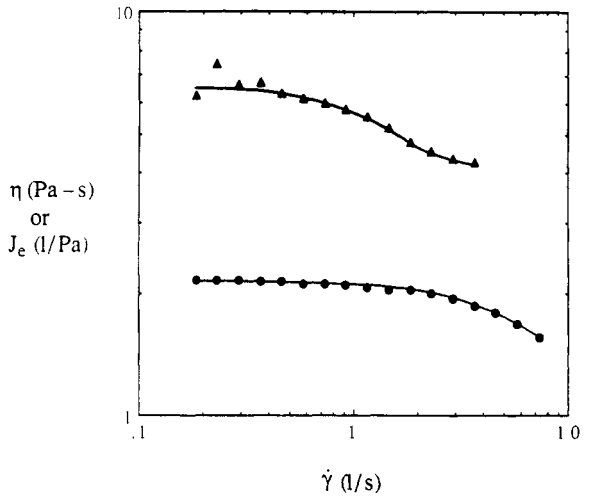

Figure 5. Viscosity η (●) and recoverable shear compliance J_e (▲) vs shear rate for 6-arm star polymer 6A at 0.118 g/mL. In order to compare the shear rate dependence in the same figure, the measured viscosity has been divided by 50 and the measured shear recoverable compliance multiplied by 5000.

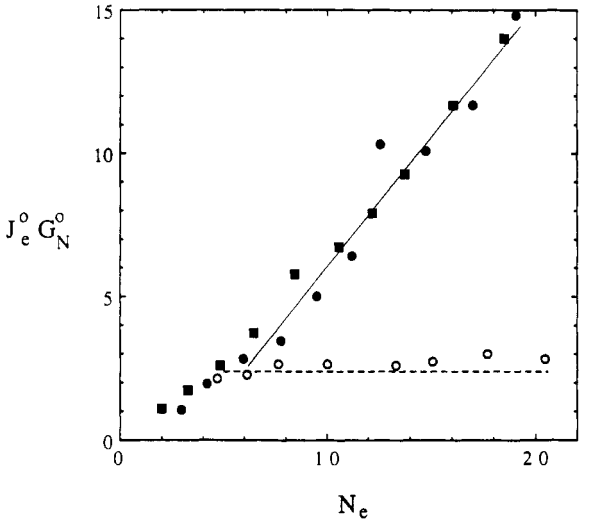

Figure 6. Product of zero shear recoverable compliance (J_e^0) and plateau modulus (G_N^0) vs number of entanglements per span (N_e). The symbols have the same meaning as in Figure 4. The dashed line gives the results measured for linear polyisoprenes in ref 15 ($J_e^0 G_N^0 \approx 2.4$). The solid line is drawn with the slope of 0.9.

a relative minimum when plotted against shear rate. This relative minimum is not apparent in Figure 5 because the occurrence of the edge fracture instability[28] prevented measurements at higher shear rates. Concentrated star polymer solutions are believed to be highly susceptible to edge fracture, as discussed in the final section of this paper.

Examination of the dependence of J_e^0 on N_e reveals a striking difference between the behavior of entangled linear polymers and entangled star polymers. At constant concentration, J_e^0 is expected to be independent of N_e for linear polymers and a linear increasing function of N_e for star polymers.[6] The difference is best revealed in a plot against N_e of the product $J_e^0 G_N^0$, where G_N^0 is the plateau modulus of polyisoprene polymers, linear or star:[6]

$$G_N^0 = 4.35 \times 10^5 \phi^{2.21} \quad (10)$$

The product $J_e^0 G_N^0$ is independent of N_e, within experimental scatter, for linear polymer LL, as shown in Figure 6. Moreover, the constant fully entangled value of $J_e^0 G_N^0$ (≈2.4) is close to that previously reported in ref 15.

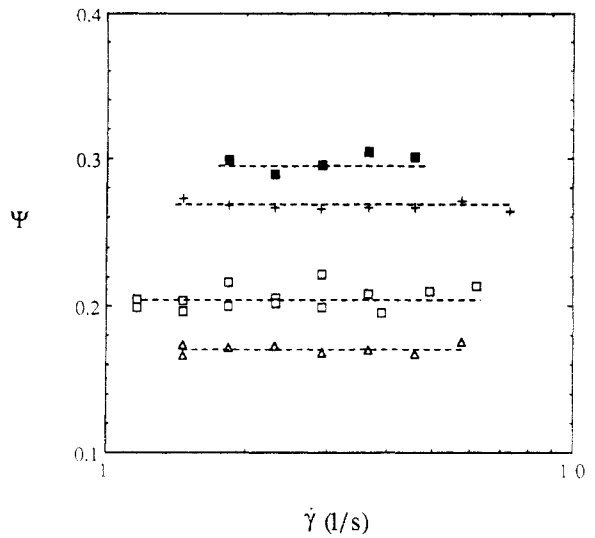

Figure 7. Shear rate dependence of the normal stress ratio Ψ. Shear rates have been shifted by a factor of 20 for star polymer 10A (C = 0.170, ■), 0.1 for star polymer 10A (C = 0.063, +) and linear polymer LH (C = 0.130, □), and 2 for linear polymer LH (C = 0.060, △).

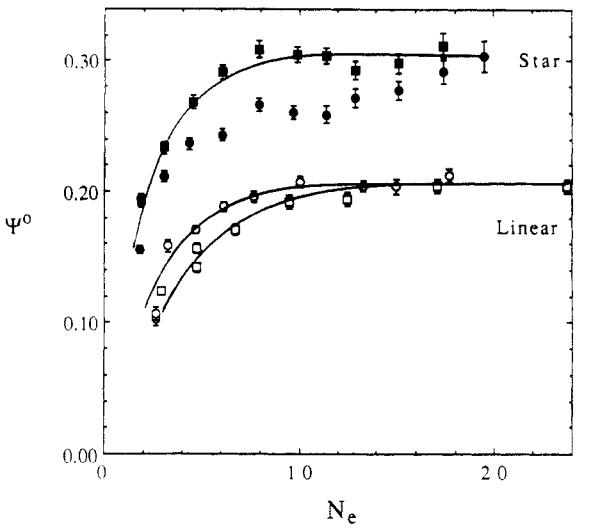

Figure 8. Normal stress ratio (Ψ^0) vs number of entanglements per span (N_e) for linear and star polyisoprenes. The symbols have the same meaning as in Figure 4.

Results for the commercially purchased linear polymer, LH, are *not* shown in Figure 6 because of the larger polydispersity of this sample. By way of contrast, the product $J_e^0 G_N^0$ is much larger than 2.4 for concentrated star polymer solutions in Figure 6. For $N_e > 8$, $J_e^0 G_N^0$ shows the expected linear dependence on N_e, signifying entrance into the enhancement concentration regime where reptation is no longer possible. However, the slope of the line in Figure 6 is somewhat greater than would be inferred from the data of ref 15. The reason for this discrepancy is unclear; it may reflect differences in the extrapolation of J_e to zero shear rate (Figure 5).

B. Second Normal Stress Difference Measurements within and below the Enhancement Regime. In the preceding section, the concentration regime within which star and linear polymers relax by different mechanisms was identified using viscosity and compliance data. Here the behavior of the second normal stress difference coefficient (Ψ_2^0) in the same concentration regime is investigated.

The difficulty in measuring Ψ_1 at low dimensionless shear rates (*Wi*) has already been discussed. Ψ_2 is even more difficult to measure than Ψ_1, and thus the estimation of Ψ_2^0 might at first glance appear to be hopelessly difficult. Fortunately, this is not the case, because the ratio $\Psi = -\Psi_2/\Psi_1$ is constant over the same shear rate range over which the individual stress coefficients are varying (Figure 7). On the basis of the data in Figure 7, we *assume* that Ψ remains constant as the zero shear limit is approached. Therefore Ψ_2^0 can be easily calculated from Ψ_1^0, and this latter quantity has already been shown to be accurately estimated, by virtue of its use in the calculation of J_e^0.

According to molecular theory,[40] Ψ^0 is close to zero (≈0.03) for dilute polymer solutions, and this prediction has been verified experimentally for a single special type of dilute solution, the so-called "Boger fluid".[35] At the other extreme, the Doi–Edwards theory[4] (with the independent alignment approximation) predicts $\Psi^0 = {}^2/_7$ for a fully entangled melt or concentrated solution of linear polymer molecules. This latter prediction has been approximately confirmed for a low-density polyethylene melt,[41] and concentrated polystyrene solutions.[42] The data presented in Figure 8 probably come closer than anything previously published to bridging the concentration gap between the dilute and fully entangled limits. Figure 8 investigates the dependence of Ψ^0 on the number of entanglements N_e, as measured for all four model polyisoprenes. First consider the linear polymer with the lowest polydispersity, polymer LL. Using criteria based on the number of entanglements per chain (eq 9),[39] polymer LL should exhibit entangled viscosity behavior for $N_e > 2$, and entangled compliance behavior for $N_e > 7$. In Figure 8, Ψ^0 appears to reach its final fully entangled value when the concentration is high enough to create about 9 entanglements per chain. The fully entangled value of Ψ^0 is 0.205 ± 0.005 for *both* linear polymers, a result which is less than the Doi–Edwards prediction, but in good agreement with recent results for polyisoprene melts.[43] Linear polymer LH appears to require about 15 entanglements per chain to reach this fully entangled limit in Figure 8. The apparent discrepancy between the number of entanglements required for full entanglement of the two linear polymers may possibly be attributed to the larger polydispersity of polymer LH, purchased commercially.

For the two star polymers, Ψ^0 has a larger value at every concentration than for either linear polymer, by an amount well in excess of the experimental uncertainty. However, linear and star polymer results in Figure 8 do appear to be converging on zero *together* at lower concentrations, in accordance with theoretical predictions.[40] Additional evidence for branching enhancement of Ψ^0 was obtained by viewing GPC chromatograms of star polymer solutions immediately after rheological measurement. Samples with a significant amount of degradation were invariably observed to exhibit Ψ^0 values substantially *lower* than the results shown in Figure 8, presumably due to the presence of linear polymer impurity. Results in Figure 8 for the 6-arm star may also have been contaminated with a slight amount of degradation, particularly at lower concentrations (i.e. the last concentrations studied chronologically). Figure 9 compares the molecular weight distribution of the 6-arm and 10-arm star polymers, both as measured after the final concentration studied. A small amount, ca. 5% of linear polymer, and also ca. 3% of a higher molecular weight component is visible in the 6-arm polymer chromatogram. This slight degradation is probably sufficiently large to account for the difference in Ψ^0 values measured for the two star polymers at lower concentrations. Therefore the high concentration limit of Ψ^0 is more reliably calculated using 10-arm star data: $\Psi^0 = 0.30 \pm 0.01$. Error bars shown in Figure 8 have been estimated from the

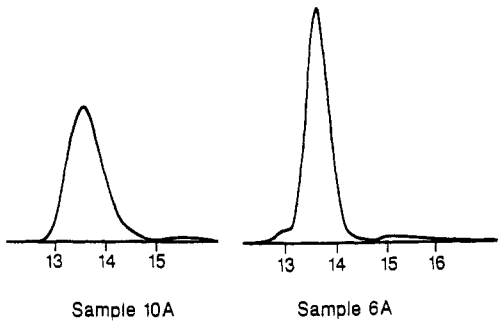

Figure 9. GPC chromatograms for 10-arm and 6-arm star polymers after final rheological measurement.

variance in Ψ values measured at different shear rates, and as such do not reflect uncertainty introduced by polymer degradation. Error bars are larger for the star polymer solutions because of their extremely long stress relaxation times at high concentrations. Experimental scatter makes it difficult to discern the number of entanglements required for full entanglement, but $N_e \approx 9$ is a reasonable estimate for both star polymers. Thus three of the four polymers appear to require about 10 entanglements over the polymer span before Ψ^0 reaches its fully entangled value.

Discussion

All three steady shear flow material functions (η_0, J_e^0, and Ψ_2^0) have been measured for two model star polymers with equal branch lengths but different branch numbers ($f = 6$ vs $f = 10$). At lower solution concentrations where the Rouse–Ham theory presumably applies, these material functions have values which are similar to the values observed for linear polymers with the same intrinsic viscosity value. The situation is quite different at concentrations high enough to create about 10 or more entanglements across the span of a polymer. In this case, all three material functions are considerably larger for star polymers than for linear polymers. The enhancement of Ψ_2^0 due to branching is the largest, because the enhancement of η_0, J_e^0, and Ψ^0 all contribute to the enhancement of Ψ_2^0: $|\Psi_2^0| = (2\Psi^0)(\eta_0^2)(J_e^0)$.

The normal stress ratio Ψ^0 is an increasing function of polymer concentration or entanglement density, as expected from molecular theory. For both of the star polymers and the best-characterized linear polymer, Ψ^0 reaches its asymptotic fully entangled value when the number of entanglements across the span of the polymer is about 10. However, the fully entangled value of Ψ^0 is larger for star polymers than for linear polymers ($\Psi^0 = 0.30 \pm 0.01$ vs 0.21 ± 0.01). This result was unexpected because the converse has been reported for polystyrene stars.[42,44] The reason for this discrepancy is not clear. It may reflect differences between polystyrene and polyisoprene, or it may reflect differences in the concentration regimes investigated. Solutions of linear polystyrenes as low in molecular weight as 37 000 were studied in ref 42, and yet Ψ^0 is reported to be independent of both concentration and molecular weight. This result is hard to understand in light of modern theories on polymer entanglement ($M_c \approx 35\,000$ for molten polystyrene[23]). Also, the viscosity of star polystyrenes is reported to have a power law dependence on entanglement density (see Figure 5 in ref 42), a result which is inconsistent with the exponential dependence on N_e predicted by theory.[6] Indirect evidence that Ψ^0 is larger for star polyisoprenes than for linear polyisoprenes comes from visual observation of the "edge fracture" flow instability in the cone-and-plate rheometer. This phenomenon initiates as an axisymmetric indentation at the air/polymer interface and is believed to be controlled by the value of N_2.[27,28] As shown elsewhere,[45] at similar values of N_1, star polyisoprene solutions fracture more readily than linear polyisoprene solutions, presumably because $\Psi^0 = -N_2/N_1$ is larger for stars.

The modified tube model based on the arm retraction relaxation mode predicts that Ψ^0 is independent of f,[26] a prediction not supported by the experimental results in Figure 8. Perhaps polymer concentrations studied here were insufficiently high to ensure the dominance of the arm retraction relaxation mode over the constraint release relaxation mode.[2] Recent results[8,11] for polybutadiene stars support the existence of a *transition* concentration regime, where reptation is impossible and relaxation occurs primarily by constraint release. This transition regime is reported to extend between $N_e = 2$ and $N_e = 12$.[11] N_e was approximately 18 at the highest concentration studied here.

Acknowledgment. We thank Nikos Hadjichristidis for some of the light-scattering results. J.W.M. thanks Hercules Inc. for the gift of the Sofica photometer and the donors of the Petroleum Research Fund, administered by the American Chemical Society, for financial support. Financial support was also provided by the CTS Division of the National Science Foundation.

References and Notes

(1) Berry, G. C.; Fox, T. G. *Adv. Polym. Sci.* **1968**, *5*, 261.
(2) Graessley, W. W. *Adv. Polym. Sci.* **1982**, *47*, 67.
(3) de Gennes, P.-G. *J. Chem. Phys.* **1971**, *55*, 572.
(4) Doi, M.; Edwards, S. F. *J. Chem. Soc., Faraday Trans. 2* **1978**, *74*, 1789, 1802, 1818; **1979**, *75*, 38.
(5) Doi, M.; Kuzuu, N. Y. *J. Polym. Sci., Polym. Lett. Ed.* **1980**, *18*, 775.
(6) Pearson, D. S.; Helfand, E. *Macromolecules* **1984**, *17*, 888.
(7) Klein, J.; Fletcher, D.; Fetters, L. J. *Nature* **1983**, *304*, 526.
(8) Bartels, C. R.; Crist, B.; Fetters, L. J.; Graessley, W. W. *Macromolecules* **1986**, *19*, 785.
(9) Shull, K. R.; Kramer, E. J.; Hadziioannou, G.; Antonietti, M.; Sillescu, H. *Macromolecules* **1988**, *21*, 2578.
(10) Lodge, T. P.; Markland, P.; Wheeler, L. M. *Macromolecules* **1989**, *22*, 3409.
(11) Shull, K. R.; Dai, K. H.; Kramer, E. J.; Fetters, L. J.; Antonietti, M.; Sillescu, H. *Macromolecules* **1991**, *24*, 505.
(12) Pearson, D. S. *Rubber Chem. Technol.* **1987**, *60*, 439.
(13) Kraus, G.; Gruver, J. T. *J. Polym. Sci.: Part A* **1965**, *3*, 105.
(14) Utracki, L. A.; Roovers, J. E. L. *Macromolecules* **1973**, *6*, 373.
(15) Graessley, W. W.; Masuda, T.; Roovers, J. E. L.; Hadjichristidis, N. *Macromolecules* **1976**, *9*, 127.
(16) Graessley, W. W.; Roovers, J. *Macromolecules* **1979**, *12*, 959.
(17) Isono, Y.; Fujimoto, T.; Inagaki, H.; Shishido, M.; Nagasawa, M. *Polym. J.* **1980**, *12*, 131.
(18) Raju, V. R.; Menezes, E. V.; Marin, G.; Graessley, W. W. *Macromolecules* **1981**, *14*, 1668.
(19) Roovers, J.; Hadjichristidis, N. *Polymer* **1985**, *26*, 1087.
(20) Roovers, J. *Polymer* **1985**, *26*, 1091.
(21) Toporowski, P. M.; Roovers, J. *J. Polym. Sci., Polym. Chem. Ed.* **1986**, *24*, 3009.
(22) Osaki, K.; Takatori, E.; Kurata, M.; Watanabe, H.; Yoshida, H.; Kotaka, T. *Macromolecules* **1990**, *23*, 4392.
(23) Ferry, J. D. *Viscoelastic Properties of Polymers*, 3rd ed.; Wiley: New York, 1980.
(24) Ham, J. S. *J. Chem. Phys.* **1957**, *26*, 625.
(25) Graessley, W. W. In *Polymers in Solution*; Forsman, W. C., Ed.; Plenum: New York, 1986; Chapter 3.
(26) Pearson, D. S. Personal communication, 1991.
(27) Larson, R. G. *Rheol. Acta* **1992**, *31*, 213.
(28) Tanner, R. I.; Keentok, M. *J. Rheol.* **1983**, *27*, 47.
(29) Bywater, S. *Adv. Polym. Sci.* **1979**, *30*, 89.
(30) Purchased from Polymer Standards Service, Mainz, Germany.
(31) Hadjichristidis, N.; Roovers, J. E. L. *J. Polym. Sci., Polym. Phys. Ed.* **1974**, *12*, 2521.
(32) Bauer, B. J.; Fetters, L. J.; Graessley, W. W.; Hadjichristidis, N.; Quack, G. F. *Macromolecules* **1989**, *22*, 2337.

(33) Bird, R. B.; Armstrong, R. C.; Hassager, O. *Dynamics of Polymeric Liquids*, 2nd ed.; Wiley: New York, 1987; Vol. 1.
(34) Baek, S. G. Ph.D. Thesis, Chemical Engineering Department, University of Utah, Salt Lake City, UT, 1991.
(35) Magda, J. J.; Lou, J.; Baek, S. G.; DeVries, K. L. *Polymer* **1991**, *32*, 2000.
(36) Magda, J. J.; Baek, S. G.; DeVries, K. L.; Larson, R. G. *Polymer* **1991**, *32*, 1794.
(37) Magda, J. J.; Baek, S. G.; DeVries, K. L.; Larson, R. G. *Macromolecules* **1991**, *24*, 4460.
(38) Zimm, B. H.; Kilb, R. W. *J. Polym. Sci.* **1959**, *37*, 19.
(39) Graessley, W. W. *Adv. Polym. Sci.* **1974**, *16*, 1.
(40) Baldwin, P. R.; Helfand, E. *Phys. Rev. A* **1990**, *41*, 6772.
(41) Meissner, J.; Garbella, R. W.; Hostettler, J. *J. Rheol.* **1989**, *33*, 843.
(42) Ramachandran, S.; Gao, H. W.; Christiansen, E. B. *Macromolecules* **1985**, *18*, 695.
(43) Rangaramanujam, K.; Kloesel, A. K.; Lai, J.; Kornfield, J. A. AIChE Annual Meeting, Los Angeles, California, Nov 17–22, 1991; Talk No. 6F.
(44) Ramachandran, S. Ph.D. Thesis, Chemical Engineering Department, University of Utah, Salt Lake City, UT, 1988.
(45) Lee, C. S.; Tripp, B. C.; Magda, J. J. *Rheol. Acta* **1992**, *31*, 306.

Registry No. Polyisoprene (homopolymer), 9003-31-0.